JACS
JOURNAL OF THE AMERICAN CHEMICAL SOCIETY
pubs.acs.org/JACS
Article

Spontaneous Reduction by One Electron on Water Microdroplets Facilitates Direct Carboxylation with CO_2

Huan Chen, Ruijing Wang, Jinheng Xu, Xu Yuan, Dongmei Zhang, Zhaoguo Zhu, Mary Marshall, Kit Bowen,* and Xinxing Zhang*

Cite This: J. Am. Chem. Soc. 2023, 145, 2647−2652
Read Online
ACCESS | Metrics & More | Article Recommendations | Supporting Information

ABSTRACT: Recent advances in microdroplet chemistry have shown that chemical reactions in water microdroplets can be accelerated by several orders of magnitude compared to the same reactions in bulk water. Among the large plethora of unique properties of microdroplets, an especially intriguing one is the strong reducing power that can be sometimes as high as alkali metals as a result of the spontaneously generated electrons. In this study, we design a catalyst-free strategy that takes advantage of the reducing ability of water microdroplets to reduce a certain molecule, and the reduced form of that molecule can convert CO_2 into value-added products. By spraying the water solution of C_6F_5I into microdroplets, an exotic and fragile radical anion, $C_6F_5I^{\bullet-}$, is observed, where the excess electron counter-intuitively locates on the σ^* antibonding orbital of the C−I bond as evidenced by anion photoelectron spectroscopy. This electron weakens the C−I bond and causes the formation of $C_6F_5^-$, and the latter attacks the carbon atom on CO_2, forming the pentafluorobenzoate product, $C_6F_5CO_2^-$. This study provides a good example of strategically making use of the spontaneous properties of water microdroplets, and we anticipate that microdroplet chemistry will be a green avenue rich in new opportunities in CO_2 utilization.

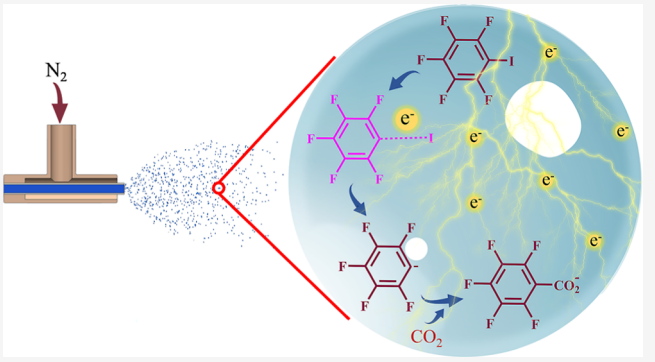

INTRODUCTION

The atmospheric carbon dioxide (CO_2) level has exceeded 400 ppm.[1] Current and projected CO_2 emissions from anthropogenic activities are leading to a continued rise in global temperatures and sea levels.[2−4] Converting CO_2 into value-added products promises to alleviate the problem,[5−7] but the challenges are obvious since CO_2 is a highly stable molecule with a high C−O bond dissociation energy (525.9 kJ/mol[8]) and a high ionization potential (317.7 kJ/mol[9]), so the direct cleavage of the C−O bond or the oxidation by one electron are both difficult. The carbon atom in CO_2 is in the highest oxidation state (+IV); as a result, it can only be activated by its reduction. Nevertheless, the direct attachment of an electron to CO_2 is also challenging, because CO_2 has a large highest-occupied molecular orbital (HOMO)−lowest unoccupied molecular orbital (LUMO) gap, making the occupation of the LUMO by an electron energetically unfavorable, and the electron affinity (EA) of CO_2 is negative (−0.6 eV).[10] So the $CO_2^{\bullet-}$ anion is metastable with a short lifetime of ∼90 ms.[10,11] As a result, despite being highly reactive, the direct use of $CO_2^{\bullet-}$ for further CO_2 fixation has been difficult and scarce.[12] Instead of directly using electrons, another strategy is to use anions or partial negative charges to attack the carbon atom on CO_2, yielding stable products with carboxylic groups.[13−20]

In recent years, water microdroplet chemistry has emerged as an exciting new field because of its ability to accelerate chemical reactions by several orders of magnitude compared to the same reactions in bulk water.[21,22] Among the unique properties of water microdroplets, an especially useful one is the observation that water microdroplets exhibit strong reducing power that can be as high as alkali metals.[23] The power of water microdroplets to promote reduction chemistry has been demonstrated in the reduction of dissolved chloroauric acid to yield gold nanoparticles and nanowires,[24] the reduction of doubly charged ethyl viologen to singly charged ethyl viologen,[25] the reduction of organic compounds by hydrogenation,[26] and the formation of the pyridyl anion in spraying an aqueous solution containing dissolved pyridine to form microdroplets.[23] It is postulated that there is a high electric field (∼10^9 V/m) at the surface of microdroplets that can pull electrons out of hydroxide ions,[27−30] resulting in an electron and a hydroxyl radical, and the electron is responsible

Received: November 29, 2022
Published: January 20, 2023

https://doi.org/10.1021/jacs.2c12731
J. Am. Chem. Soc. 2023, 145, 2647−2652

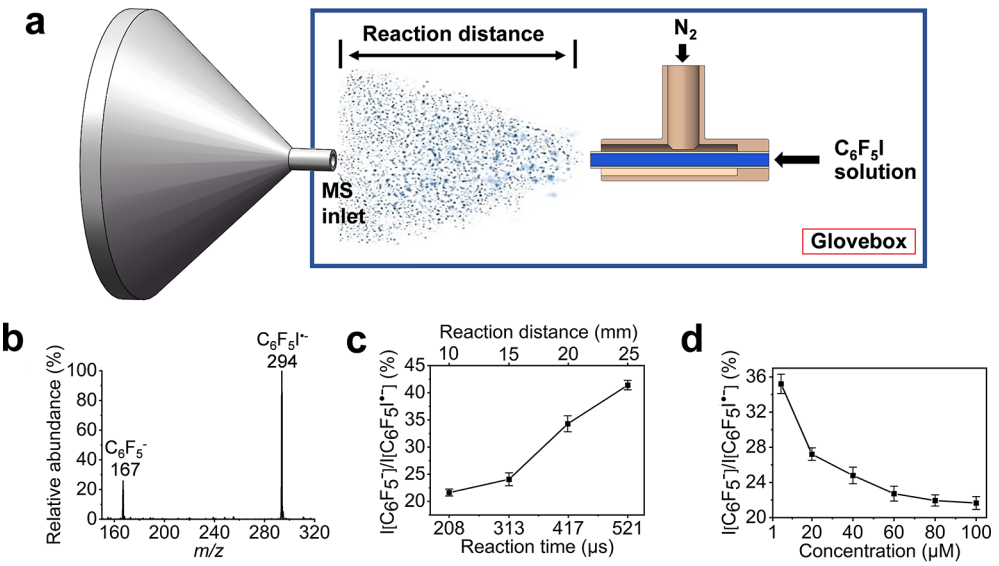

Figure 1. Spontaneous reduction of C_6F_5I in water microdroplets. (a) Experimental setup of the sprayer in a glovebox filled with pure N_2. (b) Typical mass spectrum showing the spontaneous reduction products, $C_6F_5I^{\bullet-}$ and $C_6F_5^-$. (c) $I[C_6F_5^-]/I[C_6F_5I^{\bullet-}]$ as a function of the reaction distance and reaction time when the C_6F_5I concentration is 100 μM and sheath gas pressure is 60 psi. (f) $I[C_6F_5^-]/I[C_6F_5I^{\bullet-}]$ as a function of C_6F_5I concentration when the reaction distance is 10 mm and the sheath gas pressure is 60 psi.

for the abovementioned reduction reactions,[23−26] and the hydroxyl radical can cause oxidation reactions.[31,32] In some cases, reduction and oxidation reactions occurred simultaneously.[23] The redox potential at the air−water interface has been shown to be very different from the bulk,[33] and a recent study[34] shows that on the aerial surface of air bubbles in water, the oxidation potential of OH^- to OH occurs is at least 0.7 V below redox tabled values due to the electrostatic destabilization of the hydroxide anion on water, which accelerates the formation of electrons and hydroxyl radicals at the air−water interface.

In view of the above advances, the spontaneous and strong reducing power of water microdroplets should be able to reduce and fixate CO_2. Previous studies showed that water microdroplets could convert CO_2 into formate with or without the addition of triazole as a catalyst.[35,36] In this study, we take advantage of the reducing power of water microdroplets to generate an exotic radical anion of iodopentafluorobenzene ($C_6F_5I^{\bullet-}$) by simply spraying the water solution of C_6F_5I into microdroplets in a N_2-filled glovebox. To reveal the electronic nature of this anion, a combination of gas-phase anion photoelectron spectroscopy (PES) and theoretical calculation shows that the excess electron of $C_6F_5I^{\bullet-}$ is located on the σ^* antibonding orbital of the C−I bond, unlike most radical anions with benzene rings whose excess electrons prefer to be on the π^* antibonding orbital. The electron weakens the C−I bond of C_6F_5I and forms the $C_6F_5^-$ anion, and the latter attacks the carbon atom on CO_2, forming the pentafluorobenzoate product, $C_6F_5CO_2^-$. This study brings a new strategy of CO_2 fixation by converting a molecule into its reduced form by water microdroplets, which further promotes carboxylation by attacking the C atom on CO_2.

RESULTS AND DISCUSSION

Detailed experimental methods are provided in the Supporting Information. Figure 1a presents the experimental setup. The water solutions of C_6F_5I with different concentrations are forced by a syringe pump through a fused silica capillary that sits inside a larger coaxial capillary through which high-pressure N_2 sheath gas flows. The resulting spray of microdroplets is aimed toward the inlet of a mass spectrometer. The mass spectrometer's inlet is inserted into a glovebox filled with pure N_2 (Figure 1a).[37] The distance between the end of the sprayer and the mass spectrometer inlet is defined as the microdroplet flying (reaction) distance.[38] Figure 1b presents a mass spectrum showing the spontaneous reduction products by spraying water solutions of C_6F_5I into water microdroplets. Two anionic products, $C_6F_5I^{\bullet-}$ (m/z = 294) and $C_6F_5^-$ (m/z = 167), were observed. Apparently, C_6F_5I was reduced by one electron into a radical anion, supporting the fact that electrons can easily be generated in microdroplets, and the $C_6F_5^-$ anion could be a C−I bond dissociation product from $C_6F_5I^{\bullet-}$ via a dissociative electron attachment process.[39] A same experiment performed in the atmosphere did not yield any signal related to C_6F_5I, suggesting that $C_6F_5I^{\bullet-}$ is a fragile anion that cannot survive air. To provide evidence that $C_6F_5^-$ was indeed a product from $C_6F_5I^{\bullet-}$ through C−I bond dissociation, Figure 1c shows the change of $I[C_6F_5^-]/I[C_6F_5I^{\bullet-}]$ as a function of the reaction distance and reaction time, where I denotes the mass peak intensity. By adjusting the reaction distance from 10 to 25 mm, the reaction time varied from 208 to 521 μs[38] (Figure 1c), and a clear increase of the ratio was observed, indicating that the airborne microdroplet, but not the gas phase inside the mass spectrometer, was where the reaction occurred and that $C_6F_5^-$ was a product from $C_6F_5I^{\bullet-}$. The reaction kinetics was also dependent on the concentration of C_6F_5I (Figure 1d). A higher $I[C_6F_5^-]/I[C_6F_5I^{\bullet-}]$ ratio was observed with a lower concentration. In a model study by Wilson and coworkers,[40] lower concentrations yielded higher fractions of the molecules partitioning to the microdroplet surface, suggesting that the air−water interface of the microdroplets played a key role in the reactions, which is consistent with this case and our previous studies.[25,28] The mass spectra supporting the data in Figure 1c,d are displayed in Figures S1 and S2, respectively,

https://doi.org/10.1021/jacs.2c12731
J. Am. Chem. Soc. 2023, 145, 2647−2652

and the collision-induced dissociation spectra bearing structural information of these species are provided in Figure S3.

To understand the geometric and electronic structures of $C_6F_5I^{\bullet-}$ and $C_6F_5^-$, we also performed gas-phase PES measurements and density functional theory (DFT) calculations. Detailed methods are provided in the Supporting Information. In brief, a home-built apparatus combines a laser photoemission ion source, time-of-flight mass spectrometry, and anion PES. We analyzed the kinetic energies of the resultant photoelectrons by crossing a mass-selected anion beam with a fixed-frequency photon beam. The energetics of the photodetachment process is governed by the energy-conserving relationship, $h\nu$ = EBE + EKE, where $h\nu$ is the photon energy, EBE is the electron binding (photodetachment transition) energy, and EKE is the electron kinetic energy. Figure 2 presents the photoelectron spectra of $C_6F_5^-$, I^-, and

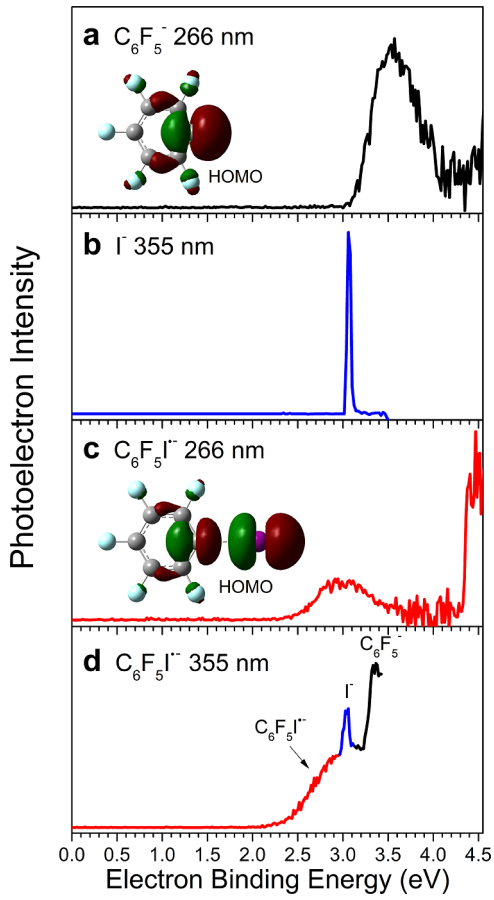

Figure 2. Photoelectron spectroscopic study of the anion species. (a) Spectrum of $C_6F_5^-$ taken with 266 nm photons. (b) Spectrum of I^- taken with 355 nm photons. (c) Spectrum of $C_6F_5I^{\bullet-}$ taken with 266 nm photons. (d) Spectrum of $C_6F_5I^{\bullet-}$ taken with 355 nm photons. The HOMOs of $C_6F_5^-$ and $C_6F_5I^{\bullet-}$ are embedded.

$C_6F_5I^{\bullet-}$ taken with different photon energies. The spectrum of $C_6F_5^-$ in Figure 2a exhibits an EBE band starting from around 3.05 eV and peaking at 3.53 eV, these two values corresponding to the EA of C_6F_5 and vertical detachment energy (VDE) of $C_6F_5^-$, in consistent with our calculated values, 3.18 and 3.50 eV, at the PBE/aug-cc-pVTZ level of theory. The spectrum of I^- in Figure 2b shows a sharp peak at 3.06 eV, corresponding to the well-known EA of iodine.[41] Figure 2c exhibits the PES of the $C_6F_5I^{\bullet-}$ parent anion using 266 nm photons. The first band starts from ~2.5 eV and peaks at 3.05 eV (VDE). The measured VDE agrees well with the calculated value, 3.12 eV, at the PBE/aug-cc-pVTZ(C,F)/aug-cc-pVTZ-PP(I) level of theory, but the onset of the first band, 2.5 eV, is not consistent with the calculated EA value, 1.59 eV. In PES experiments, only when there is enough Franck–Condon overlap between the ground state of the anion and the ground state of the neutral can EA be observed,[42] suggesting that the observed onset of the $C_6F_5I^{\bullet-}$ spectrum is not the EA due to the lack of Franck–Condon overlap (vide infra). As a result, we can only compare the calculated EA with a previous experiment, 1.48 eV, using a pulsed electron high-pressure mass spectrometer.[43] In Figure 2d, the PES of $C_6F_5I^{\bullet-}$ at 355 nm obviously has features from $C_6F_5^-$ (black), I^- (blue), and $C_6F_5I^{\bullet-}$ (red), which is a result of two-photon processes: the first photon dissociates $C_6F_5I^{\bullet-}$ into either $C_6F_5^-$ or I^-, and the second photon photodetaches them. The photodissociation suggests that the C–I bond is weakened in $C_6F_5I^{\bullet-}$ and vulnerable to 355 nm photons. The experimental and measured EA and VDE values are tabulated in Table 1 for comparison.

Table 1. Experimental and Theoretical EA and VDE Values[a]

species	expt. EA	theo. EA	expt. VDE	theo. VDE
$C_6F_5/C_6F_5^-$	3.05	3.18	3.53	3.50
I/I^-	3.06[35]			
$C_6F_5I/C_6F_5I^{\bullet-}$	1.48[37]	1.59	3.05	3.12

[a]All numbers are in eV.

As a side note, the superatom concept depicts a class of clusters and molecules that possess certain behavior akin to an atom of the periodic table.[44] EA was considered to be the defining characteristic for identifying a superatom of a halogen element. With this criterion, Al_{13} was determined to be the superatom of Br.[45] Since the EA of C_6F_5 and I are almost identical, we opine that C_6F_5 can be viewed as a superatom of I.

The calculated HOMOs of $C_6F_5^-$ and $C_6F_5I^{\bullet-}$ are embedded in Figure 2. Unlike most radical anions with benzene rings where the excess electrons prefer to be on the π^* antibonding orbital on the ring, the excess electron of $C_6F_5I^{\bullet-}$ is located on the σ^* antibonding orbital of the C–I bond, which is a singly occupied molecular orbital, making it a half bond, and elongating it from 2.09 to 2.67 Å. Such a large bond length change from neutral to anion causes a poor Franck–Condon overlap, explaining the failure of the measurement of EA in the PES experiment. This result also explains the formation of $C_6F_5^-$ by breaking the weakened C–I bond. The HOMO of $C_6F_5^-$ is an occupied sp^2 orbital located on the carbon atom, making it negatively charged by −0.38 e (Figure S4), providing a chance for attacking the carbon atom on the CO_2 molecule. The calculated geometric and charge information of these species are provided in Figure S4, and the Cartesian coordinates of all the calculated species are provided in Table S1.

We next move to the CO_2 fixation experiment taking advantage of the reducing power of water microdroplets. Figure 3a shows the mass spectrum using CO_2 as the sheath gas, and a new peak corresponding to the pentafluorobenzoate product, $C_6F_5CO_2^-$, is unambiguously observed. Remarkably, there were ~71% of the $C_6F_5^-$ anions converted into $C_6F_5CO_2^-$. The signal of $C_6F_5I^{\bullet-}$ becomes very low, suggesting

https://doi.org/10.1021/jacs.2c12731
J. Am. Chem. Soc. 2023, 145, 2647–2652

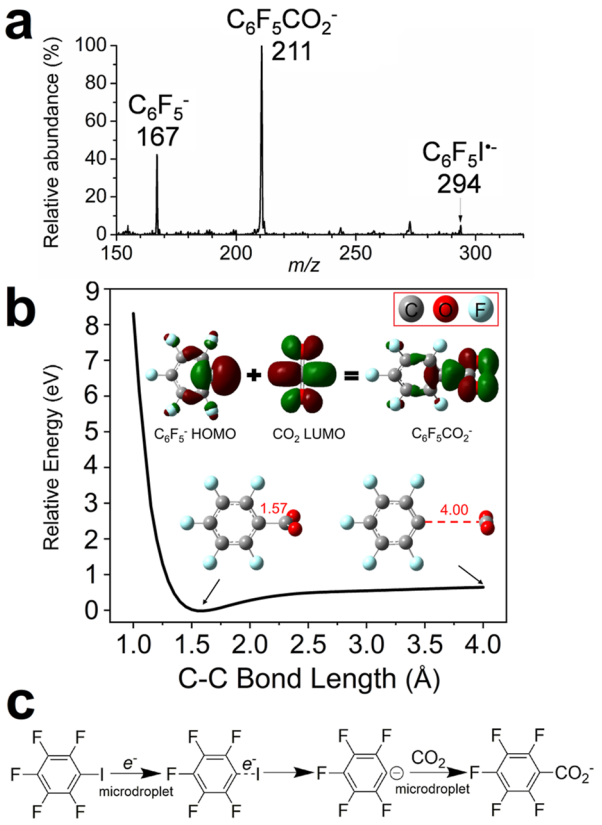

Figure 3. Fixation of CO_2 by $C_6F_5^-$ in microdroplets. (a) Mass spectrum showing the $C_6F_5CO_2^-$ product when using CO_2 as the sheath gas. (b) DFT calculation results of the potential energy surface along the C−C bond of the $(C_6F_5{-}CO_2)^-$ complex at the PBE/aug-cc-pVTZ level of theory. Typical structures along the scanned coordinate and the frontier orbitals involved in the reactions are displayed. (c) Overall reaction pathway.

that the formation of $C_6F_5CO_2^-$ was a channel consuming $C_6F_5^-$, and $C_6F_5^-$ comes from $C_6F_5I^{\bullet-}$. To better understand the reaction pathway, we performed DFT calculations at the PBE/aug-cc-pVTZ level of theory. Figure 3b plots the potential energy surface for the $(C_6F_5{-}CO_2)^-$ complex as a function of the C−C bond length with the remainder of the molecule relaxed to the ground state. There is only one potential well along the C−C coordinate, meaning that this is a barrier-free reaction. Due to the steric hindrance, the C_6F_5 moiety and the CO_2 moiety are not in the same plane. The well corresponds to the fully optimized structure with a C−C bond length of 1.57 Å. As shown in the embedded figure in Figure 3b, the symmetry of the $C_6F_5^-$ HOMO matches that of the CO_2 LUMO, explaining the barrier-free formation of the C−C bond. However, since the energy well is not large (∼1 eV), one expects this reaction to be endergonic in the gas phase due to unfavorable entropic contributions, so solvation effects in the microdroplets might have considerably stabilized the $C_6F_5CO_2^-$ product. The overall strategy of fixating CO_2 is provided in Figure 3c, and the key step is apparently using a microdroplet as a green and spontaneous electron donor.

CONCLUSIONS

To summarize, we have used spontaneously generated electrons in water microdroplets to reduce C_6F_5I into $C_6F_5I^{\bullet-}$, where the excess electron unusually occupies the σ^* antibonding orbital of the C−I bond and further breaks the bond, forming the $C_6F_5^-$ anion that fixates CO_2 into $C_6F_5CO_2^-$. This study provides an example of CO_2 utilization and brings a new catalyst-free strategy that takes advantage of the reducing power of water microdroplets for the applications of not only CO_2 fixation but also potentially a large variety of reactions such as reductive coupling and hydrogenation where the reduction by an electron plays the key role.

ASSOCIATED CONTENT

Supporting Information

The Supporting Information is available free of charge at https://pubs.acs.org/doi/10.1021/jacs.2c12731.

Experimental and theoretical methods, additional experimental, and theoretical results (PDF)

AUTHOR INFORMATION

Corresponding Authors

Kit Bowen − *Department of Chemistry, Johns Hopkins University, Baltimore, Maryland 21218, United States;* orcid.org/0000-0002-2858-6352; Email: kbowen@jhu.edu

Xinxing Zhang − *College of Chemistry, Key Laboratory of Advanced Energy Materials Chemistry (Ministry of Education), Renewable Energy Conversion and Storage Centre, Tianjin Key Laboratory of Biosensing and Molecular Recognition, Frontiers Science Centre for New Organic Matter, Nankai University, Tianjin 300071, China; Haihe Laboratory of Sustainable Chemical Transformations, Tianjin 300192, China;* orcid.org/0000-0001-5884-2727; Email: zhangxx@nankai.edu.cn

Authors

Huan Chen − *College of Chemistry, Key Laboratory of Advanced Energy Materials Chemistry (Ministry of Education), Renewable Energy Conversion and Storage Centre, Tianjin Key Laboratory of Biosensing and Molecular Recognition, Frontiers Science Centre for New Organic Matter, Nankai University, Tianjin 300071, China; Haihe Laboratory of Sustainable Chemical Transformations, Tianjin 300192, China*

Ruijing Wang − *College of Chemistry, Key Laboratory of Advanced Energy Materials Chemistry (Ministry of Education), Renewable Energy Conversion and Storage Centre, Tianjin Key Laboratory of Biosensing and Molecular Recognition, Frontiers Science Centre for New Organic Matter, Nankai University, Tianjin 300071, China; Haihe Laboratory of Sustainable Chemical Transformations, Tianjin 300192, China*

Jinheng Xu − *College of Chemistry, Key Laboratory of Advanced Energy Materials Chemistry (Ministry of Education), Renewable Energy Conversion and Storage Centre, Tianjin Key Laboratory of Biosensing and Molecular Recognition, Frontiers Science Centre for New Organic Matter, Nankai University, Tianjin 300071, China; Haihe Laboratory of Sustainable Chemical Transformations, Tianjin 300192, China; Department of Chemistry, Johns Hopkins University, Baltimore, Maryland 21218, United States*

Xu Yuan − *College of Chemistry, Key Laboratory of Advanced Energy Materials Chemistry (Ministry of Education), Renewable Energy Conversion and Storage Centre, Tianjin Key Laboratory of Biosensing and Molecular Recognition,*

Frontiers Science Centre for New Organic Matter, Nankai University, Tianjin 300071, China; Haihe Laboratory of Sustainable Chemical Transformations, Tianjin 300192, China

Dongmei Zhang − *College of Chemistry, Key Laboratory of Advanced Energy Materials Chemistry (Ministry of Education), Renewable Energy Conversion and Storage Centre, Tianjin Key Laboratory of Biosensing and Molecular Recognition, Frontiers Science Centre for New Organic Matter, Nankai University, Tianjin 300071, China; Haihe Laboratory of Sustainable Chemical Transformations, Tianjin 300192, China*

Zhaoguo Zhu − *Department of Chemistry, Johns Hopkins University, Baltimore, Maryland 21218, United States;* orcid.org/0000-0002-4395-9102

Mary Marshall − *Department of Chemistry, Johns Hopkins University, Baltimore, Maryland 21218, United States;* orcid.org/0000-0001-6614-1963

Complete contact information is available at: https://pubs.acs.org/10.1021/jacs.2c12731

Notes

The authors declare no competing financial interest.

■ ACKNOWLEDGMENTS

X.Z. acknowledges the National Natural Science Foundation of China (22174073 and 22003027), the NSF of Tianjin City (21JCJQJC00010), the Haihe Laboratory of Sustainable Chemical Transformations, the Beijing National Laboratory for Molecular Sciences (BNLMS202106), and the Frontiers Science Center for New Organic Matter at Nankai University (63181206). Portions of this material are based on work supported by the US National Science Foundation (NSF) under grant number CHE-2054308 (K.H.B.).

■ REFERENCES

(1) Hartfield, G.; et al. State of the Climate in 2017. *Bull. Am. Meteorol. Soc.* **2018**, *99*, Si-S310.

(2) Brown, P. T.; Caldeira, K. Greater Future Global Warming Inferred from Earth's Recent Energy Budget. *Nature* **2017**, *552*, 45−50.

(3) Cox, P. M.; Betts, R. A.; Jones, C. D.; Spall, S. A.; Totterdell, I. J. Acceleration of Global Warming due to Carbon-Cycle Feedbacks in a Coupled Climate Model. *Nature* **2000**, *408*, 184−187.

(4) Joos, F.; Plattner, G. K.; Stocker, T. F.; Marchal, O.; Schmittner, A. Global Warming and Marine Carbon Cycle Feedbacks on Future Atmospheric CO 2. *Science* **1999**, *284*, 464−467.

(5) Jiang, X.; Nie, X. W.; Guo, X. W.; Song, C. S.; Chen, J. G. G. Recent Advances in Carbon Dioxide Hydrogenation to Methanol via Heterogeneous Catalysis. *Chem. Rev.* **2020**, *120*, 7984−8034.

(6) Grignard, B.; Gennen, S.; Jérôme, C.; Kleij, A. W.; Detrembleur, C. Advances in the Use of CO2 as a Renewable Feedstock for the Synthesis of Polymers. *Chem. Soc. Rev.* **2019**, *48*, 4466−4514.

(7) Wang, G. X.; Chen, J. X.; Ding, Y. C.; Cai, P. W.; Yi, L. C.; Li, Y.; Tu, C. Y.; Hou, Y.; Wen, Z. H.; Dai, L. M. Electrocatalysis for CO2conversion: from fundamentals to value-added products. *Chem. Soc. Rev.* **2021**, *50*, 4993−5061.

(8) Darwent, B. d. *Bond Dissociation Energies in Simple Molecules*; National Bureau of Standards: Washington, DC, 1970.

(9) Lias, S. G. Ionization Energy Evaluation. *NIST Chemistry WebBook*; Mallard, W. G., Linstrom, P. J., Eds.; NIST Standard Reference Database Number 69; National Institute of Standards and Technology: Gaithersburg, MD, 2017.

(10) Compton, R. N.; Reinhardt, P. W.; Cooper, C. D. Collisional ionization of Na, K, and Cs by CO2, COS, and CS2: Molecular electron affinities. *J. Chem. Phys.* **1975**, *63*, 3821.

(11) Yu, D.; Rauk, A.; Armstrong, D. A. Electron Affinities and Thermodynamic Properties of Some Triatomic Species. *J. Phys. Chem.* **1992**, *96*, 6031−6038.

(12) Song, L.; Wang, W.; Yue, J.; Jiang, Y.; Wei, M.; Zhang, H.; Yan, S.; Liao, L.; Yu, D. Visible-light photocatalytic di- and hydrocarboxylation of unactivated alkenes with CO2. *Nat. Catal.* **2022**, *5*, 832−838.

(13) Zhang, X.; Lim, E.; Kim, S. K.; Bowen, K. H. Photoelectron spectroscopic and computational study of (M-CO2)(-) anions, M = Cu, Ag, Au. *J. Chem. Phys.* **2015**, *143*, 174305.

(14) Liu, G.; Ciborowski, S. M.; Zhu, Z.; Chen, Y.; Zhang, X.; Bowen, K. H. The metallo-formate anions, M(CO2)−, M = Ni, Pd, Pt, formed by electron-induced CO2 activation. *Phys. Chem. Chem. Phys.* **2019**, *21*, 10955−10960.

(15) Lim, E.; Heo, J.; Zhang, X.; Bowen, K. H.; Lee, S. H.; Kim, S. K. Anionic Activation of CO2 via (Mn-CO2)− Complex on Magic-Numbered Anionic Coinage Metal Clusters Mn- (M = Cu, Ag, Au). *J. Phys. Chem. A* **2021**, *125*, 2243−2248.

(16) Knurr, B. J.; Weber, J. M. Solvent-Driven Reductive Activation of Carbon Dioxide by Gold Anions. *J. Am. Chem. Soc.* **2012**, *134*, 18804−18808.

(17) Lee, S. H.; Kim, N.; Ha, D. G.; Kim, S. K. "Associative" Electron Attachment to Azabenzene−(CO2)n van der Waals Complexes: Stepwise Formation of Covalent Bonds with Additive Electron Affinities. *J. Am. Chem. Soc.* **2008**, *130*, 16241−16244.

(18) Graham, J. D.; Buytendyk, A. M.; Wang, Y.; Kim, S. K.; Bowen, K. H. CO2 binding in the (quinoline-CO2)− anionic complex. *J. Chem. Phys.* **2015**, *142*, 234307.

(19) Graham, J. D.; Buytendyk, A. M.; Zhang, X.; Kim, S. K.; Bowen, K. H. Carbon dioxide is tightly bound in the [Co(Pyridine)(CO2)]− anionic complex. *J. Chem. Phys.* **2015**, *143*, 184315.

(20) Oh, R.; Lim, E.; Zhang, X.; Heo, J.; Bowen, K. H.; Kim, S. K. Ab initio study on anomalous structures of anionic [(N-heterocycle)-CO2]− complexes. *J. Chem. Phys.* **2017**, *146*, 134304.

(21) Yan, X.; Bain, R. M.; Cooks, R. G. Organic Reactions in Microdroplets: Reaction Acceleration Revealed by Mass Spectrometry. *Angew. Chem., Int. Ed.* **2016**, *55*, 12960−12972.

(22) Lee, J. K.; Banerjee, S.; Nam, H. G.; Zare, R. N. Acceleration of Reaction in Charged Microdroplets. *Q. Rev. Biophys.* **2015**, *48*, 437−444.

(23) Zhao, L.; Song, X.; Gong, C.; Zhang, D.; Wang, R.; Zare, R. N.; Zhang, X. Sprayed Water Microdroplets Containing Dissolved Pyridine Spontaneously Generate Pyridyl Anions. *Proc. Natl. Acad. Sci. U.S.A.* **2022**, *119*, No. e2200991119.

(24) Lee, J. K.; Samanta, D.; Nam, H. G.; Zare, R. N. Spontaneous Formation of Gold Nanostructures in Aqueous Microdroplets. *Nat. Commun.* **2018**, *9*, 1562.

(25) Gong, C.; Li, D.; Li, X.; Zhang, D.; Xing, D.; Zhao, L.; Yuan, X.; Zhang, X. Spontaneous Reduction-Induced Degradation of Viologen Compounds in Water Microdroplets and Its Inhibition by Host-Guest Complexation. *J. Am. Chem. Soc.* **2022**, *144*, 3510−3516.

(26) Lee, J. K.; Samanta, D.; Nam, H. G.; Zare, R. N. Micrometer-Sized Water Droplets Induce Spontaneous Reduction. *J. Am. Chem. Soc.* **2019**, *141*, 10585−10589.

(27) Lee, J. K.; Walker, K. L.; Han, H. S.; Kang, J.; Prinz, F. B.; Waymouth, R. M.; Nam, H. G.; Zare, R. N. Spontaneous Generation of Hydrogen Peroxide from Aqueous Microdroplets. *Proc. Natl. Acad. Sci. U.S.A.* **2019**, *116*, 19294−19298.

(28) Zhang, D.; Yuan, X.; Gong, C.; Zhang, X. High Electric Field on Water Microdroplets Catalyzes Spontaneous and Ultrafast Oxidative C-H/N-H Cross-Coupling. *J. Am. Chem. Soc.* **2022**, *144*, 16184−16190.

(29) Mehrgardi, M. A.; Mofidfar, M.; Zare, R. N. Sprayed Water Microdroplets Are Able to Generate Hydrogen Peroxide Spontaneously. *J. Am. Chem. Soc.* **2022**, *144*, 7606−7609.

(30) Sun, Z. Y.; Wen, X.; Wang, L. M.; Ji, D. X.; Qin, X. H.; Yu, J. Y.; Ramakrishna, S. Emerging Design Principles, Materials, and Applications for Moisture-enabled Electric Generation. *eScience* **2022**, *2*, 32−46.
(31) Xing, D.; Meng, Y.; Yuan, X.; Jin, S.; Song, X.; Zare, R. N.; Zhang, X. Capture of Hydroxyl Radicals by Hydronium Cations in Water Microdroplets. *Angew. Chem., Int. Ed.* **2022**, *61*, No. e202207587.
(32) Xing, D.; Yuan, X.; Liang, C.; Jin, T.; Zhang, S.; Zhang, X. Spontaneous oxidation of I− in water microdroplets and its atmospheric implications. *Chem. Commun.* **2022**, *58*, 12447−12450.
(33) Martins-Costa, M.; Anglada, J.; Francisco, J.; Ruiz-Lopez, M. Reactivity of Atmospherically Relevant Small Radicals at the Air-Water Interface. *Angew. Chem.* **2012**, *51*, 5413−5417.
(34) Vogel, Y. B.; Evans, C. W.; Belotti, M.; Xu, L.; Russell, I. C.; Yu, L.; Fung, A. K. K.; Hill, N. S.; Darwish, N.; Gonçales, V. R.; Coote, M. L.; Swaminathan Iyer, S. K.; Ciampi, S. The Corona of a Surface Bubble Promotes Electrochemical Reactions. *Nat. Commun.* **2020**, *11*, 6323.
(35) Song, X.; Meng, Y.; Zare, R. N. Spraying Water Microdroplets Containing 1,2,3-Triazole Converts Carbon Dioxide into Formic Acid. *J. Am. Chem. Soc.* **2022**, *144*, 16744−16748.
(36) Qiu, L.; Cooks, R. G. Simultaneous and Spontaneous Oxidation and Reduction in Microdroplets by the Water Radical Cation/Anion Pair. *Angew. Chem., Int. Ed.* **2022**, *61*, No. e202210765.
(37) Zhang, D.; Lu, Y.; Wang, J.; Gong, C.; Hou, X.; Zhang, X.; Chen, J. Revisiting the Hitherto Elusive Cyclohexanehexone Molecule: Bulk Synthesis, Mass Spectrometry, and Theoretical Studies. *J. Phys. Chem. Lett.* **2021**, *12*, 9848−9852.
(38) Lai, Y.; Sathyamoorthi, S.; Bain, R. M.; Zare, R. N. Microdroplets Accelerate Ring Opening of Epoxides. *J. Am. Soc. Mass Spectrom.* **2018**, *29*, 1036−1043.
(39) Christophorou, L. G.; Stockdale, J. A. D. Dissociative Electron Attachment to Molecules. *J. Chem. Phys.* **1968**, *48*, 1956.
(40) Wilson, K. R.; Prophet, A. M.; Rovelli, G.; Willis, M. D.; Rapf, R. J.; Jacobs, M. I. A Kinetic Description of How Interfaces Accelerate Reactions in Micro-compartments. *Chem. Sci.* **2020**, *11*, 8533−8545.
(41) Hanstorp, D.; Gustafsson, M. Determination of the Electron Affinity of Iodine. *J. Phys. B: At., Mol. Opt. Phys.* **1992**, *25*, 1773.
(42) Wang, W.; Marshall, M.; Collins, E.; Marquez, S.; Mu, C.; Bowen, K. H.; Zhang, X. Intramolecular Electron-Induced Proton Transfer and Its Correlation with Excited-State Intramolecular Proton Transfer. *Nat. Commun.* **2019**, *10*, 1170.
(43) Dillow, G. W.; Kebarle, P. Substituent effects on the electron affinities of perfluorobenzenes C6F5X. *J. Am. Chem. Soc.* **1989**, *111*, 5592−5596.
(44) Luo, Z.; Castleman, A. W. Special and General Superatoms. *Acc. Chem. Res.* **2014**, *47*, 2931−2940.
(45) Bergeron, D. E.; Castleman, A. W.; Morisato, T.; Khanna, S. N. Formation of Al 13 I - : Evidence for the Superhalogen Character of Al 13. *Science* **2004**, *304*, 84−87.

https://doi.org/10.1021/jacs.2c12731
J. Am. Chem. Soc. 2023, 145, 2647−2652